

SMART MICELLAR SYSTEMS FOR BRAIN DRUG DELIVERY



Y. Islam¹, A. Leach¹, C. Coxon¹, J. Downing¹, M. Platt², S. Pluchino³, T. Ehtezazi¹

¹School of Pharmacy and Biomolecular Sciences, James Parsons Building, Byrom Street, Liverpool, L3 3AF

²Department of Chemistry, Loughborough University, Loughborough LE11 3TU, United Kingdom

³Department of Clinical Neurosciences, Centre for Brain Repair, University of Cambridge, Robinson Way CB2 0PY, UK.



1. INTRODUCTION:

➤ Neurodegenerative disorders (like dementia, MS, PD, AD, stroke and traumatic brain injury) cost directly to healthcare system over £134 billion per annum in the UK and USA. These disorders affect the quality of life of the patient.

➤ Brain matrix metalloproteinase-9 (MMP-9) levels increase in neurodegenerative disorders. An enzyme that plays an important role in many pathological processes of brain injuries and inflammation.

The Challenge

➤ Conventional drug delivery systems have number of limitations such as route of administration (intracranial injection), bioavailability (permeability across the BBB), and the safety of the carrier material.

Our approach

➤ We aim to develop a **safe and smart material** that forms a micellar drug delivery system with the ability to target the brain specifically and release a payload at the suitable region. Our approach is to apply state-of-the-art integrated experimental and computational methods to identify the smart enzyme responsive materials (Figure 1).

➤ The key advantages of our smart biomaterial are; permeability across the BBB and being responsive to MMP-9.

2. METHODS:

➤ Experimental data was analysed by applying statistical models; Lamort, Kridel, Kcat/KM and Ratnikov datasets in relation to MMP-9 cleavable peptides.

➤ Molecular docking was applied to identify MMP-9 cleavable peptides with desired sensitivity.

➤ Synthesis of suitable peptides using a CEM Liberty Blue synthesizer, and characterization via Liquid chromatography–mass spectrometry (LC-MS).

➤ Conjugation of Cholesteryl chloroformate with peptide, using N,N-Diisopropylethylamine (DIPEA) and Dimethylformamide (DMF).

➤ Characterizing the self-assembled nano-micelles using transmission electron microscopy (TEM).

Table 1. A list of known MMP-9 substrates, processed using statistical techniques to assign cleavability scores.

Sequence	Probability	Lamort	Ratnikov	Kridel	Kcat/KM	Y_Score
KAG-LLC	4.3636		0.47	-0.11	251	0.18
KG-LC	8.22765		0.47		358	0.47
SGRR-LLSRTA	0.51	3.61	0.50	0.12	1,200	1.41
RPLA-LWRSQ	4.12	4.03	0.69	0.49	2,000	1.74
RGLA-LWRSQ	0.36	3.37	0.56	0.47	2,000	1.47
GPLL-LEEAQ	29.73	4.06	0.55	0.45	2,000	1.69
EAAPSS-VIAATE	24.05	4.13	0.53	0.46	2,000	1.71
SGLRPAK-STA	23.23	3.74	0.64	0.00	5,800	1.46
PLG-LEEA	46.53	3.87	0.66	0.46	8,000	1.66
GPOG-IAGQ	1449.48	4.00	0.62	0.27	8,400	1.63
SGOPHY-LTTA	27.00	3.84	0.65	0.37	8,800	1.62
IPES-LRAG	38.64	4.07	0.66	0.36	12,600	1.70
SGFGSRY-LTA	52.20	3.76	0.63	0.11	13,200	1.50
GPLG-LERAQ	160.15	4.11	0.62	0.51	14,000	1.75
GAMF-LEAIP	6.26	4.06	0.60	0.26	15,000	1.64
RPLA-LEESQ	4.08	3.99	0.60	0.44	21,000	1.68
KPAG-LLGC	191.40	4.08	0.62	0.45	24,000	1.72
SGPLF-YSVTA	11.48	4.10	0.67	0.37	25,600	1.71
PLA-LWRSQ	5.64	4.03	0.68	0.49	51,000	1.73
SGPRA-VSTTA	74.98	4.17	0.65	0.35	61,000	1.72
RPLG-LEEA	34.02	3.86	0.66	0.46	62,000	1.66
RPLE-LWRSQ	1.59	4.02	0.63	0.45	67,000	1.70
SGKIPRT-LTA	52.94	4.16	0.68	0.20	67,500	1.68
RPLG-LGAAQ	237.75	4.23	0.74	0.38	133,000	1.78
RPLA-LWEEQ	9.19	3.96	0.71	0.39	143,000	1.69
GPLG-LREAQ	566.23	4.15	0.71	0.50	160,000	1.79
SGKIPRR-LTA	29.81	4.09	0.72	0.18	160,000	1.66
SGKGRQ-ITA	170.54	4.15	0.65	0.23	188,000	1.68
RPLA-LWESQ	5.67	3.99	0.69	0.49	198,000	1.72
RPLG-LGGAQ	638.64	4.24	0.74	0.38	270,000	1.79
RPLA-LRRSQ	7.63	4.12	0.69	0.44	291,000	1.75
RPLG-LWGAAQ	482.56	4.19	0.74	0.51	750,000	1.81

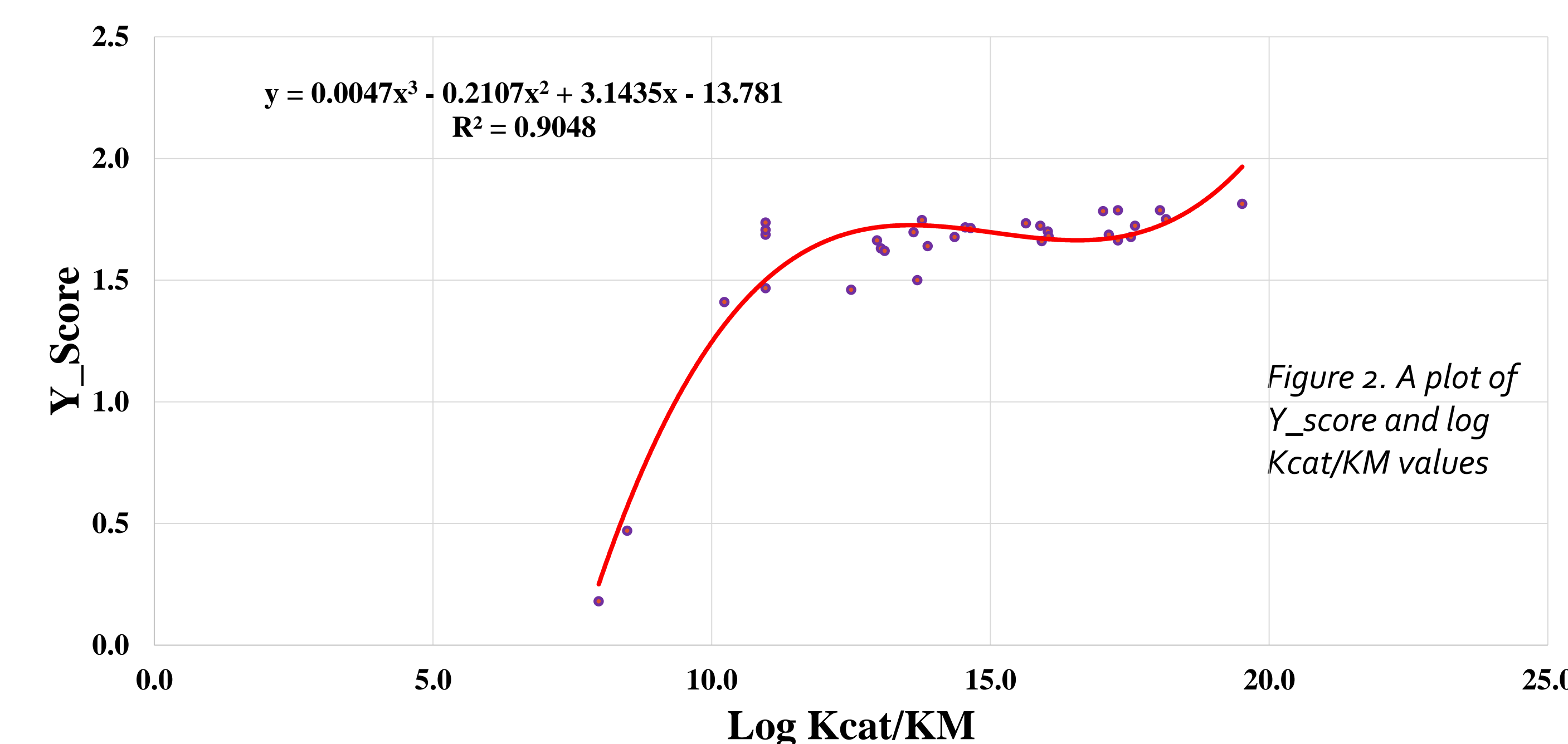


Figure 2. A plot of Y_score and log Kcat/KM values

3. RESULTS:

➤ Y_scores were calculated as average of Lamort, Ratnikov and Kridel for literature known sequences (Table 1).

➤ Y_score against log Kcat/KM values of known peptides gave a polynomial regression curve with $R^2 = 0.9048$ (Figure 2).

➤ The frequency distribution of amino acids in natural materials that are responsive to MMP-9 is shown in Figure 3. This identifies key features of known substrates.

➤ Figure 4 shows how a good substrate for MMP-9 is predicted to be accommodated in the enzyme active site. This provides an explanation for many of the preferences shown in Figure 3.

➤ Table 2 presents a list of novel MMP-9 cleavable peptides with predicted Y_score and Kcat/KM. These are from a database of 1.2 million MMP-9 cleavable peptides that were generated by applying the above statistical and molecular modelling techniques.

➤ TEM image of self-assembled nano-micelle with MMP-9 cleavable peptide and a short rabies virus glycoprotein (sRVG) shuttle peptide (Figure 5). The size of nano-micelles ranged from 50-200 nm.

Table 2. Novel MMP-9 cleavable peptides with predicted cleavability (Kcat/KM)

Sequence	Y_score	Kcat/KM
PFM-AG	2.59	1,462,495
PFR-AG	2.51	1,264,381
PFR-LG	2.04	405,685
PKR-LG	2.03	389,159
PFR-FG	2.00	345,901

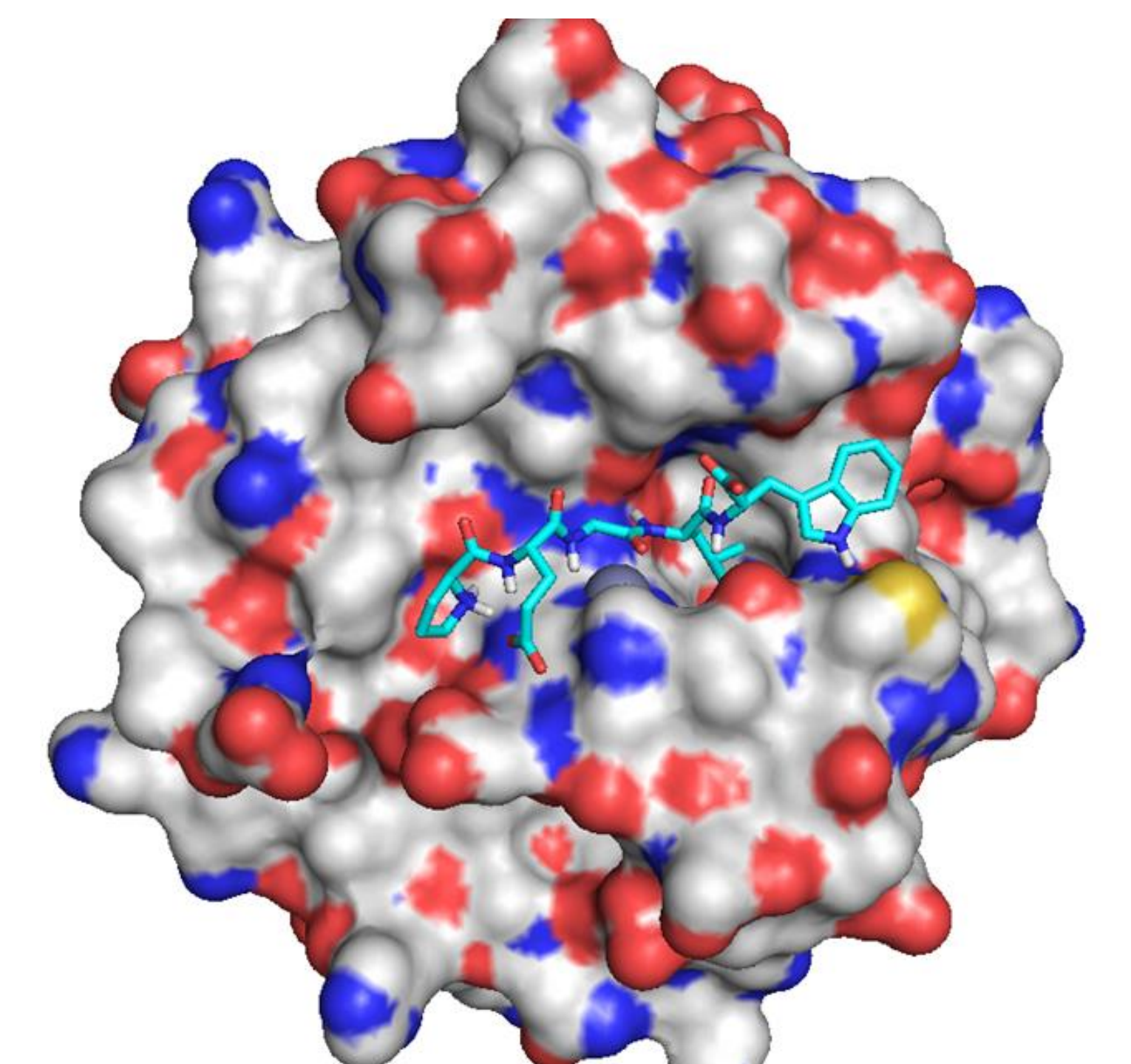


Figure 4. Characterising suitable biomaterial by docking using a structure of the enzyme taken from the protein databank. A peptide (PEGLW) after autodocking is shown in cyan; it can be observed that "Leu" extends into the S1' pocket and "Trp" wraps around the bridge over the S1' pocket.

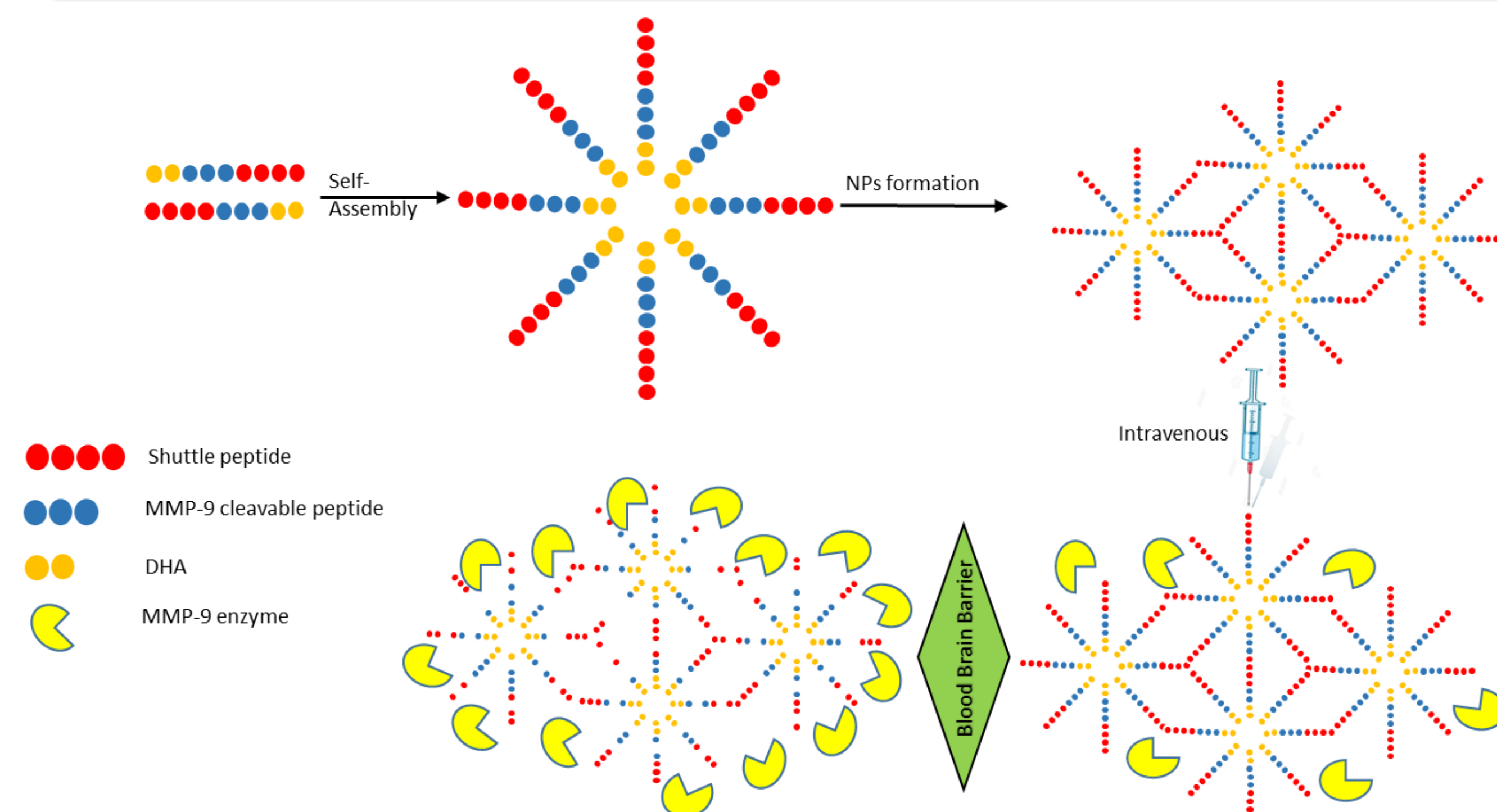


Figure 1. Schematic presentation of the core of the smart biomaterial and mechanism of action of Smart-MMP-9 Responsive drug delivery system..

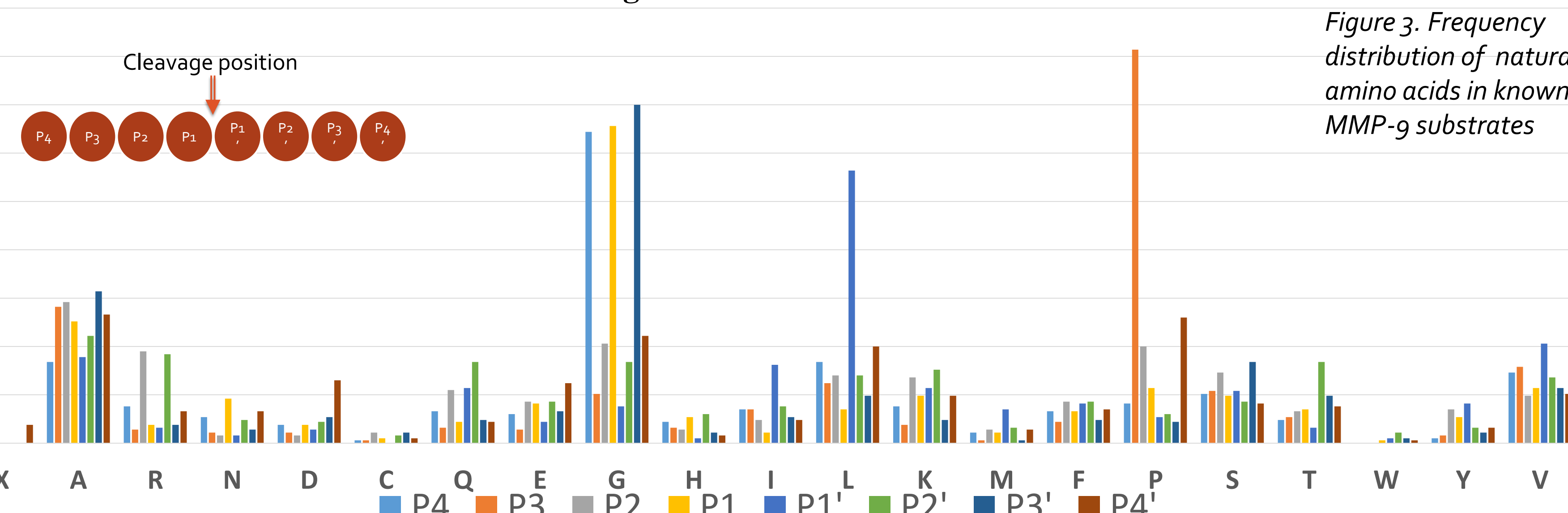


Figure 3. Frequency distribution of natural amino acids in known MMP-9 substrates

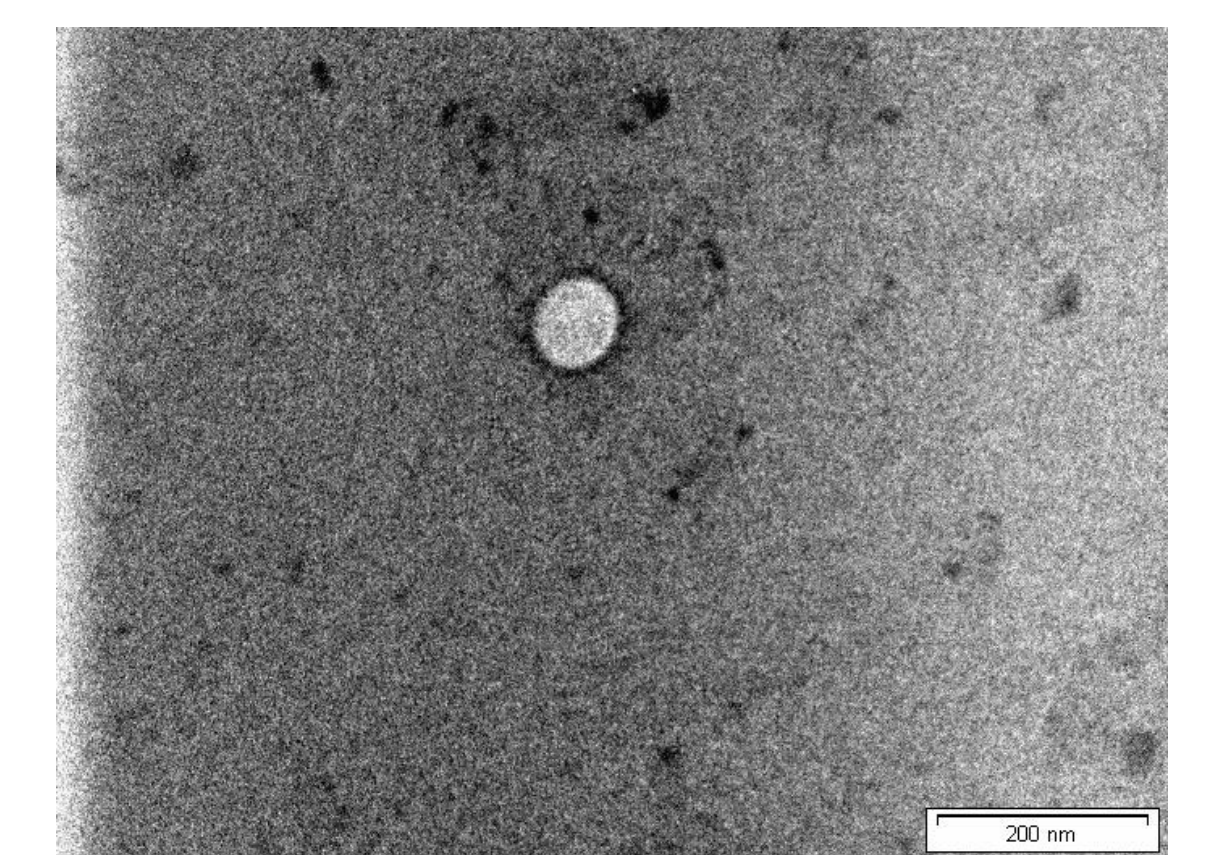


Figure 5. TEM image of MMP-9 nano-micelle with targeting ligand

4. CONCLUSIONS:

➤ Novel MMP-9 cleavable peptides were generated by applying computational methods.

➤ Self assembled nano-micelles were formulated with MMP-9 cleavable and brain targeting peptides.